In Situ Growth of Silver Nanoparticles on Graphene Quantum Dots for Ultrasensitive Colorimetric Detection of H2O2 and Glucose

ARTICLE *in* ANALYTICAL CHEMISTRY · MAY 2014

Impact Factor: 5.64 · DOI: 10.1021/ac501497d · Source: PubMed

4 AUTHORS, INCLUDING:

Shuai Chen
Northeastern University (Shenyang, China)
13 PUBLICATIONS **214** CITATIONS
SEE PROFILE

Xu-Wei Chen
Northeastern University (Shenyang, China)
79 PUBLICATIONS **1,720** CITATIONS
SEE PROFILE

analytical chemistry

Article

pubs.acs.org/ac

In Situ Growth of Silver Nanoparticles on Graphene Quantum Dots for Ultrasensitive Colorimetric Detection of H_2O_2 and Glucose

Shuai Chen,[†,‡] Xin Hai,[†] Xu-Wei Chen,*[,†] and Jian-Hua Wang*[,†,§]

[†]Research Center for Analytical Sciences, Northeastern University, Box 332, Shenyang 110819, China

[‡]College of Life and Health Sciences, Northeastern University, Shenyang, 110819, China

[§]Collaborative Innovation Center of Chemical Science and Engineering, Tianjin, 300071, China

Supporting Information

ABSTRACT: We report a facile green approach for in situ growth of silver nanoparticles (AgNPs) on the surface of graphene quantum dots (GQDs). GQDs serve as both reducing agent and stabilizer, and no additional reducing agent and stabilizer is necessary. The GQDs/AgNPs hybrid exhibits a superior absorbance fading response toward the reduction of H_2O_2. A simple colorimetric procedure is thus proposed for ultrasensitive detection of H_2O_2 without additional chromogenic agent. It provides a record detection limit of 33 nM for the detection of H_2O_2 by the AgNPs-based sensing system. This colorimetric sensing system is further extended to the detection of glucose in combination with the specific catalytic effect of glucose oxidase for the oxidation of glucose and formation of H_2O_2, giving rise to a detection limit of 170 nM. The favorable performances of the GQDs/AgNPs hybrid are due to the peroxidase-like activity of GQDs.

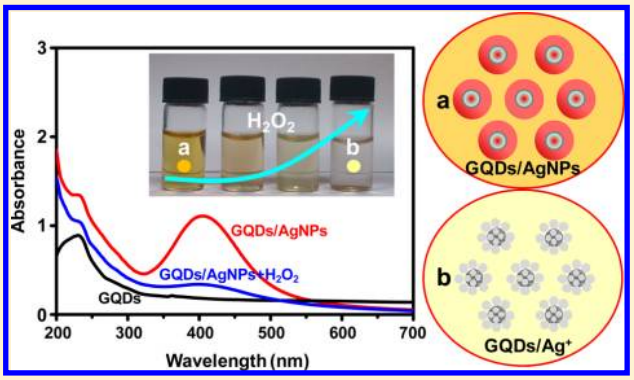

Silver nanoparticles (AgNPs) are widely used as antibacterial agents. The improvement in the performance of multifunctional AgNPs has always been an important issue in nanoscience and nanotechnology.[1] The stabilization of AgNPs is a challenging topic in practical applications due to their features of ease of oxidation and aggregation. The use of stabilizing agents has been demonstrated to be an effective strategy for this purpose. A variety of materials have been successfully employed to enhance the stability and antibacterial activity of AgNPs, including biologically friendly polymer poly(*N*-vinyl-2-pyrrolidone) and poly(vinyl alcohol), organic small molecules (b-cyclodextrin-4,40-dipyridine inclusion complex), silicon nanowires, ZnO, and TiO_2 NPs, as well as multiwalled carbon nanotubes.[1−4]

Graphene and graphene oxide (GO) have attracted attention due to their outstanding electronic, mechanical, and chemical properties. These unique features make them quite popular in constructing graphene (or graphene oxide)/metal-NPs hybrids, showing great potentials for catalysis,[5,6] surface-Raman scattering,[7] antibacteria agent,[8,9] electron transport system,[10] hydrogen generation,[11] optical and chemical sensing.[12] The fabrication of a graphene/AgNPs hybrid also exhibits a recognized effect on enhancing the stability of AgNPs.[13] A $Ag(NH_3)_2OH$-based one-step photochemical reaction method was developed for specific preparation of graphene oxide/AgNPs composites with uniformly deposited AgNPs. It was demonstrated that the composites are highly dispersible and stable in water in the absence of any stabilizing agent.[14]

Graphene quantum dots (GQDs) are zero-dimensional graphene sheets with lateral sizes less than 100 nm. Besides the property of photoluminescence contributed by quantum confinement and edge effects, GQDs are also merited with numerous novel chemical/physical properties including low cytotoxicity, excellent solubility, and convenience for surface grafting, making them quite attractive in optoelectronic devices, photovoltaic and light emitting, bioimaging, sensors, and electrochemical catalysis.[15−19] It has been demonstrated that the structure and morphology of Ag/graphene composites contribute greatly to its superior electrical properties on the reduction of H_2O_2.[20] It was reported that the AgNPs/F-SiO_2/GO composite exhibits favorable catalytic performance on H_2O_2 reduction, giving rise to a sensitive electrochemical strategy for the assay of H_2O_2.[21]

In the present study, we propose a facile approach for the preparation of GQDs/AgNPs hybrid via in situ growth of AgNPs on the surface of GQDs (Scheme 1). In this process, GQDs act as an excellent stabilizer, which ensures that the GQDs/AgNPs hybrid is stable within at least 7 days. The obtained GQDs/AgNPs hybrid exhibits an improved catalytic effect toward the reduction of H_2O_2. The conversion of AgNPs to Ag^+ leads to a sensitive color fading, providing a colorimetric

Received: April 23, 2014
Accepted: May 26, 2014
Published: May 26, 2014

   dx.doi.org/10.1021/ac501497d | *Anal. Chem.* 2014, 86, 6689−6694

Scheme 1. Preparation of GQDs/AgNPs Hybrid and the Scheme for H_2O_2 and Glucose Detection Based on Color Fading of the Hybrid

method for the ultrasensitive detection of H_2O_2 and glucose using GQDs/AgNPs as an optical sensor.

EXPERIMENTAL SECTION

Reagents and Materials. High purity graphite powder (spectral grade), P_2O_5, $K_2S_2O_8$, H_2SO_4 (concentrated), $KMnO_4$, $AgNO_3$, H_2O_2 (30%), $NH_3{\cdot}H_2O$ (28%), glucose oxidase (GOx, EC 1.1.3.4), glucose (Glu), fructose (Fru), lactose (Lac), sucrose (Suc), maltose (Mat), and mannose (Man) are obtained from Sinopharm Chemical Reagent Co., Ltd. (Shanghai, China). All solutions are prepared with ultrapure water of 18.2 MΩ cm^{-1}. Britton–Robinson buffer (BR buffer, pH 5.0) is prepared by a mixture of 0.04 M H_3BO_3, 0.04 M H_3PO_4 and 0.04 M CH_3COOH. The pH value of the buffer is adjusted by titrating with 0.2 M NaOH and controlled by an Orion 818 pH meter (Thermo Fisher Scientific, U.S.A.).

Preparation of GQDs. GO is prepared from natural graphite powder according to the Hummers and Offeman method,[22] where the graphite powder is preoxidized by using P_2O_5, $K_2S_2O_8$, and concentrated H_2SO_4 before use.

GQDs are prepared as described in our previous studies.[23,24] Briefly, 5 mL of GO aqueous solution (50 mg mL^{-1}) and 20 mL of HNO_3 (65%, v/v) are sealed into a Teflon vessel and heated at 200 °C for 5 min under microwave irradiation (at 800W and 30 MPa). After cooling the reaction mixture to temperature, GQDs are obtained by rotary evaporation.

Preparation of GQDs/AgNPs Hybrid. One hundred milliliters of GQDs solution (0.5 mg mL^{-1}) is adjusted to pH 7 by ammonium hydroxide, followed by ultrasonication for 20 min. Tollens's reagent is freshly prepared by the addition of ammonium hydroxide (28%) into 1 mL of $AgNO_3$ (50 mg mL^{-1}) solution drop-wise to form $Ag(NH_3)_2OH$. The above two solutions are fully mixed under vigorous stirring for 30 min, and then the reaction mixture is heated at 100 °C for 60 min. The final product, consisting of a purplish red GQDs/AgNPs hybrid solution, is obtained. The GQDs/AgNPs hybrid is stable at room temperature for 1 week. For the purpose of comparison, GO/AgNPs hybrid is prepared by following the same method, except for replacing the GQDs with GO.

Characterization of GQDs/AgNPs Hybrid. Transmission electron microscopy (TEM) images are obtained with a field-emission transmission electron microscope with an EDS spectrometer at an accelerating voltage of 200 kV (JEM-2100F, JEOL, Ltd., Japan). FT-IR spectra are recorded on Nicolet-6700 FT-IR spectrophotometer (Thermo Fisher, U.S.A.) from 400 to 4000 cm^{-1}. XPS measurements are performed by using an ESCALAB 250 surface analysis system (Thermo Fisher, U.S.A.). XRD patterns are recorded on an X'Pert Pro MPD X-ray diffractometer (PW 3040/60, PANalytical B.V., Holland) with Cu Kα irradiation (λ = 1.5406 Å). UV–vis absorption spectra are recorded with a U-3900 UV–vis spectrophotometer (Hitachi High Technologies, Japan) with a 0.5 cm quartz cell and a bandwidth setting of 2 nm at a scan speed of 1200 nm min^{-1}.

Colorimetric Assay of H_2O_2 and Glucose. The detection of H_2O_2 is conducted by the following procedure: 100 μL of the as-prepared GQDs/AgNPs hybrid solution (0.1 mg mL^{-1}), 100 μL of BR buffer (40 mM), and 400 μL of H_2O_2 solution within a range of 0–100 μM are added sequentially into a 1.5 mL tube. The reaction mixture is then incubated at room temperature for 5 min, and the absorption spectra in the range of 300–700 nm are recorded. A_0 and A represent the absorbance of GQDs/AgNPs hybrid in the absence and presence of H_2O_2, respectively.

For the detection of glucose, a mixture containing 300 μL of glucose sample solution and 100 μL of GOx (1.0 mg mL^{-1}) is first incubated at 37 °C for 30 min. Afterward, 100 μL of the GQDs/AgNPs hybrid solution (0.1 mg mL^{-1}) and 100 μL of BR buffer (40 mM) are added, and the mixture is further incubated at 37 °C for another 30 min. The absorption spectra are recorded as described in the above section.

Comparing Catalytic Activities of GQDs/AgNPs and GO/AgNPs Hybrids. Ten microliters of GQDs/AgNPs hybrid

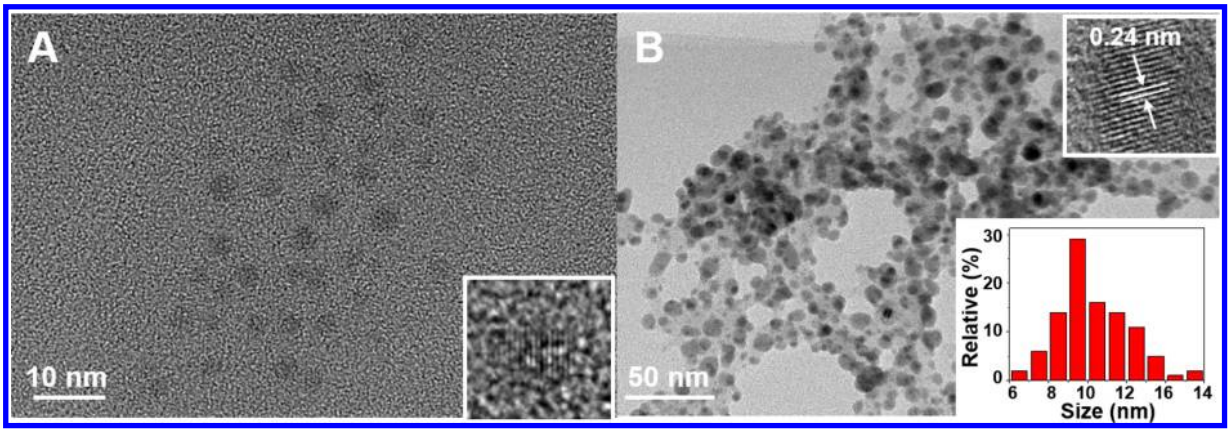

Figure 1. TEM images of GQDs (A) and the GQDs/AgNPs hybrid (B).

dx.doi.org/10.1021/ac501497d | Anal. Chem. 2014, 86, 6689–6694

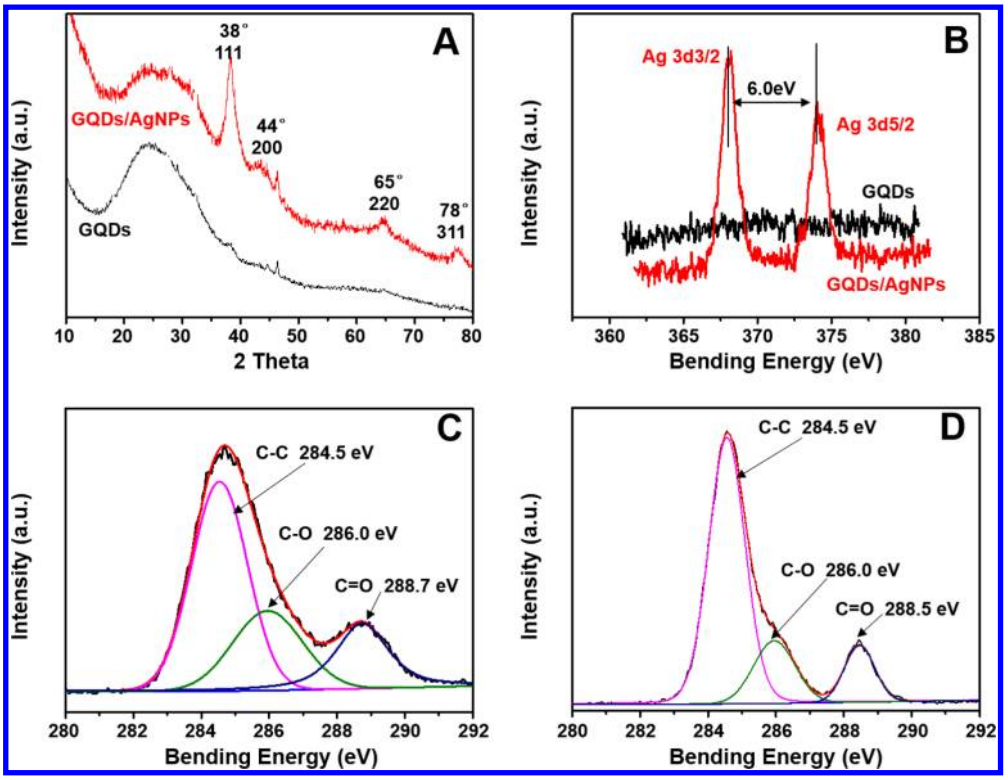

Figure 2. XRD patterns of GODs and the GODs/AgNPs hybrid (A), Ag 3d XPS spectra of GODs and the GODs/AgNPs hybrid (B), C 1s XPS spectra of GODs (C), and C 1s XPS spectra of the GODs/AgNPs hybrid (D).

(1 mg mL^{-1}) is added into a 1.0 mL solution containing 1.0 mM H_2O_2 and 0.5 mM TMB (3,3′,5,5′-tetramethylbenzidine) in the presence of 0.2 M acetate buffer (at pH 3.0). The variations in the characteristic absorption of oxidized TMB at 652 nm with time are recorded. For the case of GO/AgNPs hybrid system, a similar procedure is performed and an absorption−time curve is recorded for the purpose of comparison.

RESULTS AND DISCUSSION

Characterization of GQDs/AgNPs Hybrid. The morphologies of GQDs and the GQDs/AgNPs hybrid are characterized by HRTEM, as illustrated in Figure 1. It shows that the average size of GQDs is 2−3 nm (Figure 1A), consistent with that reported in the literature.[25] In the present study, $Ag(NH_3)_2OH$ is used as the precursor and the cationic moiety of $Ag(NH_3)_2^+$, which is prone to adsorb onto the surface of GQDs under electrostatic interaction, as there are an abundance of hydroxyl and carboxylic groups on the surface and edge of GQDs.[14] GQDs have been recognized as excellent electron transporters, rendering them to be optimal candidates for performing as electrochemical-sensing materials.[26] Under a moderate temperature of 100 °C, the thermal reduction of GQDs[27] facilities the formation of $Ag^0(NH_3)_2$ on the surface of GQDs.[10] The $Ag^0(NH_3)_2$ is temporarily stable in the presence of free NH_3 which serves as electron donor, while it is prone to agglomerate into oligomeric clusters and will eventually grow into colloidal AgNPs.[28] The formed colloidal AgNPs provide improved surface for the adsorption of $Ag(NH_3)_2^+$, which further facilities the reduction of GQDs and the ensuing in situ growth of AgNPs onto the surface of GQDs. It could be clearly seen that the size of the final GQDs/AgNPs hybrid after a 60 min reaction ranges from 6 to 15 nm, which is obviously larger than that of the bare GQDs (ca. 2−3 nm). The outerplanar spacing for the lattice fringes is 0.24 nm (Figure 1B, inset), corresponding to the [111] lattice plane of the Ag crystal.[5,10] The energy dispersive spectrum further proves the formation of AgNPs in the final product (Figure S1).

Figure 2A shows the typical XRD profiles of GQDs and the GQDs/AgNPs hybrid. GQDs exhibit a broader (002) peak centered at 2θ of 24.36°. The interlayer spacing is 0.365 nm, larger than the *d*-spacing (0.335 nm) for the pristine graphite (2θ = 26.6°).[29,30] For the GQDs/AgNPs hybrid, the (002) peak shifts to a higher degree at 2θ of 24.75°, corresponding to a smaller interlayer spacing of 0.359 nm. The decrement of interlayer spacing should be ascribed to the decrease of oxygen-containing groups on the surface of GQDs induced by the thermal reduction. Besides, the peaks at 2θ = 38°, 44°, 65°, and 78° are the characteristic bands of (111), (200), (220), and (311) crystalline planes of Ag,[20,31] suggesting the formation of pure crystalline Ag on the GQDs surface. The slitting of the 3d doublet of Ag is deduced to be 6.0 eV (Figure 2B), which agrees well with the theoretic value of the metallic silver.

It is known that GQDs are merited with excellent stability and hydrophilicity due to the abundant hydroxyl and carboxylic groups on their surfaces and edges.[25,32] The existence of −COOH group on the surface of the as-prepared GQDs are evident by C 1s XPS (Figure 2C). The three main types of C 1s peaks at 284.5, 286.0, and 288.7 eV on the XPS spectra of GQDs are assigned to C−C, C−O, and C═O, respectively. However, for the case of the GQDs/AgNPs hybrid, a decrease on the intensity of the C−O peak is observed (Figure 2D). This indicates the reduction of C−O groups on GQDs by the in situ growth of AgNPs. FT-IR spectra further confirmed the reduction of C−O group. As illustrated in Figure S2, the absorption band of C−O group at 1128 cm^{-1} almost disappears

dx.doi.org/10.1021/ac501497d | *Anal. Chem.* 2014, 86, 6689−6694

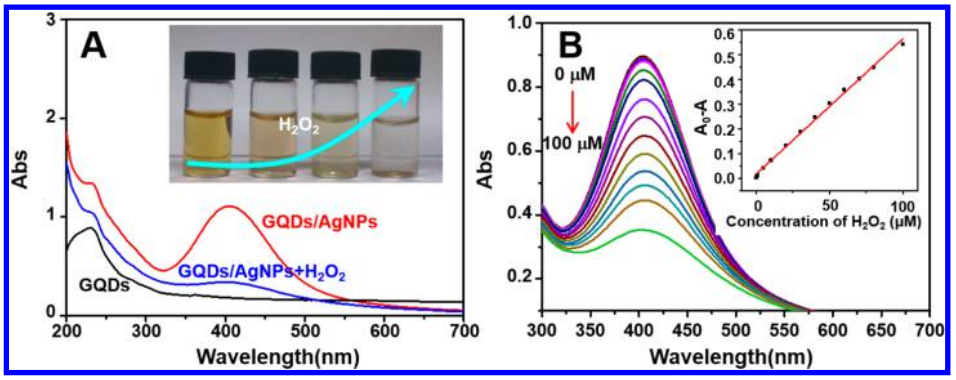

Figure 3. (A) UV−vis absorption spectra of 0.02 mg mL^{-1} GQDs, 0.02 mg mL^{-1} GQDs/AgNPs hybrid, and 0.02 mg mL^{-1} GQDs/AgNPs + 100 μM H_2O_2 system. Inset: photographs of GQDs/AgNPs hybrid solution in the presence of 0, 10, 100, and 1000 μM H_2O_2; (B) UV−vis absorption spectra of GQDs/AgNPs hybrid in the presence of 0, 0.1, 0.5, 1.0, 5, 10, 20, 30, 40, 50, 60, 70, 80, and 100 μM H_2O_2. Inset: plot of absorbance decrease versus H_2O_2 concentration (0.1−100 μM).

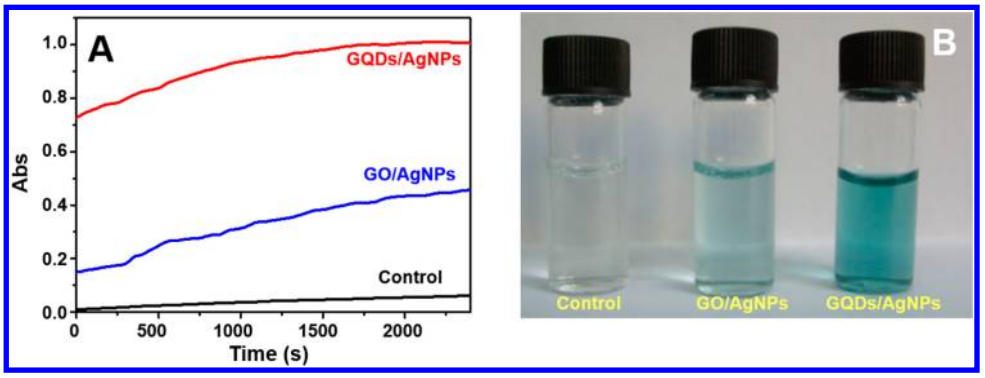

Figure 4. (A) Time-dependent absorbance of TMB solution (0.5 mM) at 652 nm in the presence of 1000 μM H_2O_2. (B) Photographs of TMB solution after oxidation by H_2O_2 and under the catalysis of GQ/AgNPs (0.01 mg mL^{-1}) and GODs/AgNPs hybrids (0.01 mg mL^{-1}).

in the FT-IR spectrum of GQDs/AgNPs hybrid. The reduction of oxygen-containing functional groups also leads to a decrease in the intensity of O 1s XPS signals (Figure S3), indicating the improved stability of the GQDs/AgNPs hybrid by the hybridization between the AgNPs and the sp^2 dangling bonds at the defect sites of GQDs.[33]

Colorimetric Detection of H_2O_2. Figure 3A illustrates that GQDs display a maximum absorption at 230 nm and a shoulder band at ca. 300 nm, attributed to the $\pi-\pi^*$ transition of aromatic sp^2 domains and $n-\pi^*$ transition of C═O. It is clearly shown that in situ growth of AgNPs on the surface of GODs results in a new absorption band at 405 nm. This is the characteristic absorption of AgNPs induced by surface plasmon absorption, offering a yellowish solution of the GQDs/AgNPs hybrid. Our experiments further indicated that obvious color fading for the GODs is observed in the presence of H_2O_2, and the extent of color fading increases with the concentration of H_2O_2 (Figure 3A, Inset). This observation provides a potential for quantitative detection of H_2O_2. In order to achieve the best performance for H_2O_2 detection, we have scrutinized the effects of some important parameters, including the concentration of $AgNO_3$ and GQDs, the volume of $NH_3{\cdot}H_2O$ solution, the reaction temperature, and the reaction time. The results are shown in Figure S4. For further studies, the optimal parameters listed in Table S1 are adopted for the preparation of the GODs/AgNPs hybrid.

Figure 3B shows the UV−vis absorption spectra of the GQDs/AgNPs hybrid in the presence of various amounts of H_2O_2 under the above optimal conditions. A linear calibration graph is achieved by plotting $(A_0 - A)$ versus H_2O_2 concentration within a range of 0.1−100 μM (R^2 = 0.996), deriving a detection limit of 33 nM. In comparison with some previously reported electrochemical, fluorimetric, and colorimetric procedures for H_2O_2 detection, the present colorimetric approach exhibits a record sensitivity, that is, at least a 10-fold improvement in the sensitivity over the reported AgNPs-based procedures, as shown in Table S2.

In the present system, the color fading is attributed to the oxidation of AgNPs in the presence of H_2O_2 as an oxidant,[34,35] which may proceed through the reaction of AgNPs and H_2O_2 ($Ag^0 + 2H_2O_2 \rightarrow Ag^+ + O_2^{\bullet-} + 2H_2O$). As is shown in Figure 3, the decrease in the surface plasmon resonance band of AgNPs at 405 nm corresponds to the concentration of H_2O_2. Furthermore, peroxidase can effectively catalyze the oxidation reaction, which helps to improve the sensitivity. The aromatic basal plan structure and the surface carboxylic groups offer GO significant peroxidase-like activity,[36] whereas the nanometer-sized GQDs sheets are proved to exhibit higher activity than the micrometer-sized GO sheets, as GODs have more intact aromatic structure and are rich in periphery carboxylic groups.[37] In the present study, the catalytic oxidation of TMB in the presence of H_2O_2 is adopted to evaluate the catalytic ability of GQDs/AgNPs and GO/AgNPs hybrids by monitoring the characteristic absorbance of TMB oxide at 652 nm. As shown in Figure 4, fast colorimetric responses (i.e., less than 2 s) are observed for both GO/AgNPs and GQDs/AgNPs hybrids. This observation is comparable to an amperometric response of GO/AgNPs hybrid toward the reduction of H_2O_2.[21] It is clearly

dx.doi.org/10.1021/ac501497d | Anal. Chem. 2014, 86, 6689−6694

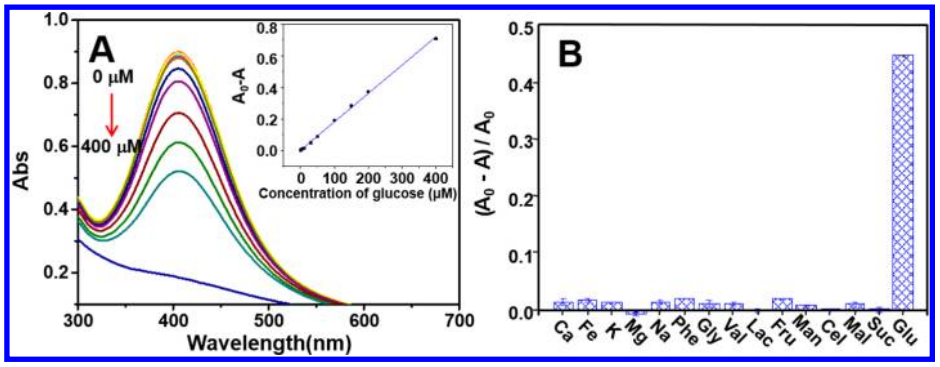

Figure 5. (A) Absorption spectra of GQDs/AgNPs (0.017 mg mL^{-1}) at different glucose concentrations: 0, 0.5, 3, 5, 10, 30, 50, 100, 150, 200, and 400 μM. Inset: plot of absorbance decrease versus glucose concentration (0.5−400 μM). (B) Absorbance decrease of the GQDs/AgNPs hybrid (0.017 mg mL^{-1}) in the presence of 200 μM glucose and other carbohydrates as well as metal cations.

shown that the GQDs/AgNPs hybrid exhibits much more sensitive response than that of the GO/AgNPs hybrid.

Colorimetric Detection of Glucose. It is known that GOx can specifically catalyze the oxidation of glucose in the presence of oxygen to form H_2O_2.[34] By combining this reaction with the GQDs/AgNPs hybrid, highly sensitive detection of glucose is feasible based on the color fading of the GQDs/AgNPs hybrid associated with the produced H_2O_2. After optimizing the experimental parameters, a linear calibration graph is achieved by plotting the absorbance decrease versus glucose concentration within 0.5−400 μM (R^2 = 0.999), deriving a detection limit of 170 nM (Figure 5A). Table S3 compares the analytical performance of the present glucose sensing system with some of the reported procedures for glucose detection. The GODs/AgNPs hybrid system is much more sensitive than the reported electrochemical, fluorimetric, and colorimetric approaches. It is especially worth mentioning that a 760-fold improvement on the sensitivity is achieved by using the GQDs/AgNPs hybrid system with respect to a similar colorimetric protocol based on bare AgNPs. On the other hand, Figure 5B shows the fading response of GQDs/AgNPs hybrid toward glucose and some other carbohydrates as well as metal cations at the level of 0.2 mM. It indicates that the GQDs/AgNPs-based detection system exhibits a specific response to glucose due to the substrate specificity of GOx. This provides an excellent selectivity in the fabrication of glucose biosensor based on GQDs/AgNPs hybird.

CONCLUSIONS

The facile preparation of stable GQDs/AgNPs hybrid is reported by use of $Ag(NH_3)_2OH$ as the precursor and GQDs as the substrate. GQDs act as both the reducing agent and stabilizer for the reduction of silver at moderate temperature. In situ growth of AgNPs onto the surface of GQDs facilitates favorable dispersion of the nanoparticles and improves their stability in aqueous medium. The obtained GQDs/AgNPs hybrid exhibits improved fading response toward the reduction of H_2O_2 due to the enhanced peroxidase catalytic activity of GQDs. It further facilitates ultrasensitive colorimetric detection of H_2O_2. Combination of the GQDs/AgNPs hybrid system with the specific catalytic effect of GOx for the oxidation of glucose results in the development of a highly sensitive sensing system for glucose. The observation described in the present study provides a new avenue for the development of a highly sensitive biosensing system.

ASSOCIATED CONTENT

Supporting Information

The energy-dispersive spectra, FT-IR spectra, and XPS spectra of the hybrid material, as well as sensing performances of the analytical system. This material is available free of charge via the Internet at http://pubs.acs.org..

AUTHOR INFORMATION

Corresponding Authors

*E-mail: (X.-W.C.) chenxuwei@mail.neu.edu.cn.
*E-mail: (J.-H.W.) jianhuajrz@mail.neu.edu.cn. Fax: +86-24-83676698. Tel: +86-24-83688944.

Notes

The authors declare no competing financial interest.

ACKNOWLEDGMENTS

Financial support from National Natural Science Foundation of China (21275027, 21235001), the Program of New Century Excellent Talents in University (NCET-11-0071), and Fundamental Research Funds for the Central Universities (N110805001, N130105002, and N130105002) are highly appreciated.

REFERENCES

(1) Chernousova, S.; Epple, M. *Angew. Chem., Int. Ed.* **2013**, *52*, 1636−1653.
(2) Vijayaraghavan, K.; Nalini, S. P. K. *Biotechnol. J.* **2010**, *5*, 1098−1110.
(3) Jiang, X.; Yu, A. *J. Nanosci. Nanotechnol.* **2010**, *10*, 7829−7875.
(4) Montazer, M.; Shamei, A.; Alimohammadi, F. *Prog. Org. Coat.* **2012**, *75*, 379−385.
(5) Li, Q.; Qin, X.; Luo, Y.; Lu, W.; Chang, G.; Asiri, A. M.; Al-Youbi, A. O.; Sun, X. *Electrochim. Acta* **2012**, *83*, 283−287.
(6) Jeon, E. K.; Seo, E.; Lee, E.; Lee, W.; Um, M. K.; Kim, B. S. *Chem. Commun.* **2013**, *49*, 3392−3394.
(7) Zhou, Y.; Cheng, X.; Yang, J.; Zhao, N.; Ma, S.; Li, D.; Zhong, T. *RSC Adv.* **2013**, *3*, 23236−23241.
(8) Wu, M.; Lu, D.; Zhao, Y.; Ju, T. *Micro Nano Lett.* **2013**, *8*, 82−85.
(9) Jiang, B.; Tian, C.; Song, G.; Chang, W.; Wang, G.; Wu, Q.; Fu, H. *J. Mater. Sci.* **2013**, *48*, 1980−1985.
(10) Tang, X. Z.; Cao, Z. w.; Zhang, H. B.; Liu, J.; Yu, Z. Z. *Chem. Commun.* **2011**, *47*, 3084−3086.
(11) Yang, L.; Luo, W.; Cheng, G. *ACS Appl. Mater. Inter.* **2013**, *5*, 8231−8240.
(12) Sun, Z.; Dong, N.; Wang, K.; Koenig, D.; Nagaiah, T. C.; Sanchez, M. D.; Ludwig, A.; Cheng, X.; Schuhmann, W.; Wang, J.; Muhler, M. *Carbon* **2013**, *62*, 182−192.

(13) Zhang, Z.; Zhang, J.; Zhang, B.; Tang, J. *Nanoscale* **2013**, *5*, 118−123.
(14) Zhang, Y.; Yuan, X.; Wang, Y.; Chen, Y. *J. Mater. Chem.* **2012**, *22*, 7245−7251.
(15) Lin, L.; Rong, M.; Luo, F.; Chen, D.; Wang, Y.; Chen, X. *TrAC, Trends Anal. Chem.* **2014**, *54*, 83−102.
(16) Yan, X.; Li, B.; Li, L. S. *Acc. Chem. Res.* **2013**, *46*, 2254−2262.
(17) Li, L.; Wu, G.; Yang, G.; Peng, J.; Zhao, J.; Zhu, J. J. *Nanoscale* **2013**, *5*, 4015−4039.
(18) Zhang, Z. P.; Zhang, J.; Chen, N.; Qu, L. T. *Energy Environ. Sci.* **2012**, *5*, 8869−8890.
(19) Shen, J.; Zhu, Y.; Yang, X.; Li, C. *Chem. Commun.* **2012**, *48*, 3686−3699.
(20) Zhang, F. J.; Zhang, K. H.; Xie, F. Z.; Liu, J.; Dong, H. F.; Zhao, W.; Meng, Z. D. *Appl. Surf. Sci.* **2013**, *265*, 578−584.
(21) Lu, W.; Luo, Y.; Chang, G.; Sun, X. *Biosens. Bioelectron.* **2011**, *26*, 4791−4797.
(22) Hummers, W. S.; Offeman, R. E. *J. Am. Chem. Soc.* **1958**, *80*, 1339−1339.
(23) Chen, S.; Liu, J. W.; Chen, M. L.; Chen, X. W.; Wang, J. H. *Chem. Commun.* **2012**, *48*, 7637−7639.
(24) Chen, S.; Hai, X.; Xia, C.; Chen, X. W.; Wang, J. H. *Chem.—Eur. J.* **2013**, *19*, 15918−15923.
(25) Tien, H. W.; Huang, Y. L.; Yang, S. Y.; Wang, J. Y.; Ma, C. C. M. *Carbon* **2011**, *49*, 1550−1560.
(26) Wu, Y.; Zhou, J.; Fishkin, N.; Rittmann, B. E.; Sparrow, J. R. *J. Am. Chem. Soc.* **2011**, *133*, 849−857.
(27) Wei, Z.; Wang, D.; Kim, S.; Kim, S. Y.; Hu, Y.; Yakes, M. K.; Laracuente, A. R.; Dai, Z.; Marder, S. R.; Berger, C.; King, W. P.; de Heer, W. A.; Sheehan, P. E.; Riedo, E. *Science* **2010**, *328*, 1373−1376.
(28) Texier, I.; Rémita, S.; Archirel, P.; Mostafavi, M. *J. Phys. Chem.* **1996**, *100*, 12472−12476.
(29) Peng, J.; Gao, W.; Gupta, B. K.; Liu, Z.; Romero-Aburto, R.; Ge, L.; Song, L.; Alemany, L. B.; Zhan, X.; Gao, G.; Vithayathil, S. A.; Kaipparettu, B. A.; Marti, A. A.; Hayashi, T.; Zhu, J. J.; Ajayan, P. M. *Nano Lett.* **2012**, *12*, 844−849.
(30) Guo, H. L.; Wang, X. F.; Qian, Q. Y.; Wang, F. B.; Xia, X. H. *ACS Nano* **2009**, *3*, 2653−2659.
(31) Yuan, W.; Gu, Y.; Li, L. *Appl. Surf. Sci.* **2012**, *261*, 753−758.
(32) Ma, J.; Zhang, J.; Xiong, Z.; Yong, Y.; Zhao, X. S. *J. Mater. Chem.* **2011**, *21*, 3350−3352.
(33) Ran, X.; Sun, H.; Pu, F.; Ren, J.; Qu, X. *Chem. Commun.* **2013**, *49*, 1079−1081.
(34) Wen, T.; Qu, F.; Li, N. B.; Luo, H. Q. *Anal. Chim. Acta* **2012**, *749*, 56−62.
(35) Tashkhourian, J.; Hormozi-Nezhad, M. R.; Khodaveisi, J.; Dashti, R. *Sens. Actuators, B* **2011**, *158*, 185−189.
(36) Song, Y. J.; Qu, K. G.; Zhao, C.; Ren, J. S.; Qu, X. G. *Adv. Mater.* **2010**, *22*, 2206−2210.
(37) Zhang, Y.; Wu, C.; Zhou, X.; Wu, X.; Yang, Y.; Wu, H.; Guo, S.; Zhang, J. *Nanoscale* **2013**, *5*, 1816−1819.